J Mater Sci (2016) 51:10160–10165

Few-layer thick WS_2 nanosheets produced by intercalation/exfoliation route

Feng Huang[1,2], JiKang Jian[1,2,*], and Rong Wu[2]

[1] School of Physics and Optoelectronic Engineering, Guangdong University of Technology, Guangzhou 510006, China
[2] Department of Physics, Xinjiang University, Urumqi 830046, China

Received: 27 April 2016
Accepted: 20 July 2016
Published online: 26 July 2016

ABSTRACT

Thin two-dimensional (2D) nanostructures of layered materials are of importance for both science and technology due to their unique properties and promising applications. Few-layer tungsten disulfide (WS_2) presents some amazing optoelectronic behaviors that have attracted great interest. In this work, WS_2 nanosheets with few-layer (<10 layers) thickness have been successfully produced by Li ions intercalation/exfoliation of bulk WS_2 via a solvothermal technique. X-ray diffraction indicates that hexagonal crystal structure of bulk WS_2 remains the same after the intercalation/exfoliation treatment. Scanning electron microscopy and transmission electron microscopy characterizations reveal that the exfoliated products are single-crystalline thin nanosheets with high crystallinity. Atomic force microscopy reveals that 8-layer thick WS_2 nanosheets can be fabricated by the present approach. Raman phonon modes of the prepared WS_2 nanosheets present the redshifts due to their decreased thickness. The work provides a facile and affective route to high-quality WS_2 thin 2D nanostructures that would have great potentials for optoelectronics.

Introduction

Two-dimensional (2D) nanostructure of carbon, i.e., graphene, has inspired great interesting in the last decade because of its unique structure and physical properties [1–4]. Meanwhile, as the analogues of graphene, some atomically thick 2D nanostructures of layered inorganic compounds, such as transition metal dichalcogenides (TMDs, including MoS_2, WS_2, WSe_2, TiS_2, etc.), transition metal oxides (TMOs, including MoO_3, WO_3, etc.), and hexagonal boron nitride (h-BN), have drawn considerable attention from both fields of sciences and technologies [1, 5–8]. These 2D nanostructures present unique physical and chemical properties, and some applications in optoelectronics and photonics have already been demonstrated [9, 10].

Among those materials, it is known that hexagonal 2H-WS_2 has typical layered structure in which each layer consists of a plane of tungsten atoms between two close-packed planes of sulfur atoms [11]. Bulk WS_2 is a narrow band semiconductor with an indirect band gap of 1.35 eV that limits its applications in optoelectronics, while a direct band gap can be

Address correspondence to E-mail: jianjikang@126.com

DOI 10.1007/s10853-016-0243-7

achieved in 2D monolayer WS_2 [12–14], which makes great change in its physical properties and enables it to possess a series of potential applications [15, 16]. Nowadays, some reports have shown that 2D WS_2 can be obtained by different methods including direct pyrolysis [17], atmospheric pressure chemical vapor deposition [18], thermal reduction sulfurization [19], chemical exfoliation [20], modified L-cysteine-assisted solution-phase method [21], and so on.

For layer-structured compounds, it is reasonable to expect that the exfoliation approaches are simple and effective to realize their 2D nanostructures. In particular, Li-ion-assisted wet chemical intercalation/exfoliation method has been successfully used to fabricate a series of layered materials. Zhong et al. developed a hydrothermal Li intercalation and exfoliation route using ethylene glycol as both reductant and solvent to obtain ultrathin Bi_2Te_3 nanosheets from Bi_2Te_3 bulk [22]. Similarly, the ultrathin MoS_2 nanosheets with good quality and high yield were produced [15]. Xie et al. reported that freestanding five-atom-thick Bi_2Se_3 single layers were first synthesized via a scalable intercalation/exfoliation strategy [23]. Using *n*-butyllithium as intercalation precursor, Rao's group synthesized WS_2 layers by a 72-h intercalation treatment in hexane solvent under N_2 atmosphere and ultrasonication [6].

In this work, we report the fabrication of two-dimensional WS_2 thin nanosheets by Li-ion intercalation/exfoliation route [23]. Li ions were intercalated in bulk WS_2 through a solvothermal technique, and the 2D WS_2 nanosheets were finally obtained by the exfoliation process using sonication treatment. The phase, morphology, microstructure, and Raman scattering of the obtained products were characterized. The results show that the as-prepared WS_2 nanosheets are well-crystallized single crystals and their thickness can be down to 8-layer WS_2. Compared with the previous reports on liquid or chemical exfoliation of WS_2 [6, 20], the present method is low cost and facile because no dangerous *n*-butyllithium or supercritical CO_2 was involved. The work provides an effective route to high-quality WS_2 thin layers with promising applications in optoelectronics.

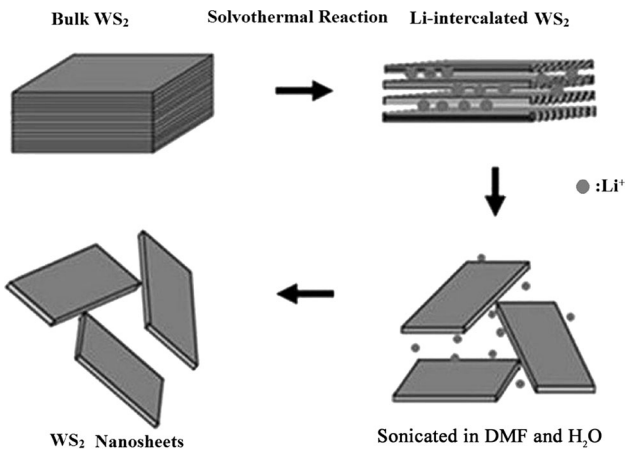

Figure 1 Schematic illustration of the formation of WS_2 nanosheets.

Experimental procedure

Materials preparation

The starting materials, commercial available WS_2 (99 wt%) and Li_2CO_3 (99 wt%) powders, were directly used without further purification. The synthesis of the WS_2 nanosheets involves two steps, i.e., Li intercalation and exfoliation procedures, which is similar with the previous report [23]. In a typical run, 352 mg WS_2 powders and 142 mg Li_2CO_3 were mixed and put into a Teflon-lined stainless-steel autoclave with the capacity of 50 mL. Then 40 mL benzyl alcohol was added into the autoclave and vigorously stirred for 60 min. After that, the autoclave was sealed and maintained at 200 °C for 48 h. Cooled to room temperature naturally, the precipitates, i.e., Li-intercalated WS_2, were collected at the bottom of the autoclave and repeatedly rinsed by deionized (DI) water, acetone, and alcohol to remove soluble inorganic and organic impurities. Then the Li-intercalated WS_2 were dried at 50 °C for 6 h in vacuum. 30 mg Li-intercalated WS_2, 30 mL distilled water, and 30 mL dimethyl formamide (DMF) were added into a jar with a capacity of 125 mL, which was sealed and sonicated at for 12 h. The resultant dispersions were centrifuged at 600 rpm for 30 min and then the supernatant was collected. After centrifuging the supernatant at 6000 rpm for 10 min, the collected products were orderly washed with 3 % HCl and DI water to remove the residual Li_2CO_3. Finally, the as-prepared products were collected by repeatedly washing with ethanol and drying at 50 °C for 6 h in vacuum.

Characterization of the materials

The final products were characterized by X-ray diffraction (XRD), scanning electron microscopy

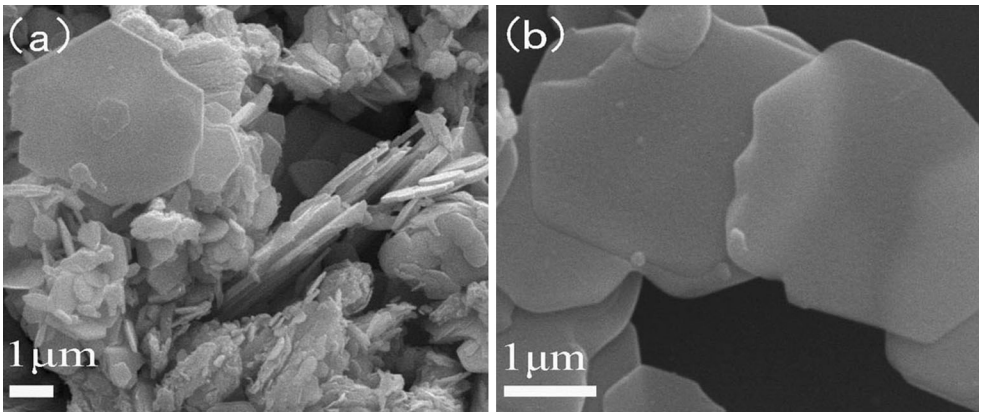

Figure 2 SEM images of WS_2 bulk (**a**) and the exfoliated WS_2 nanosheets (**b**).

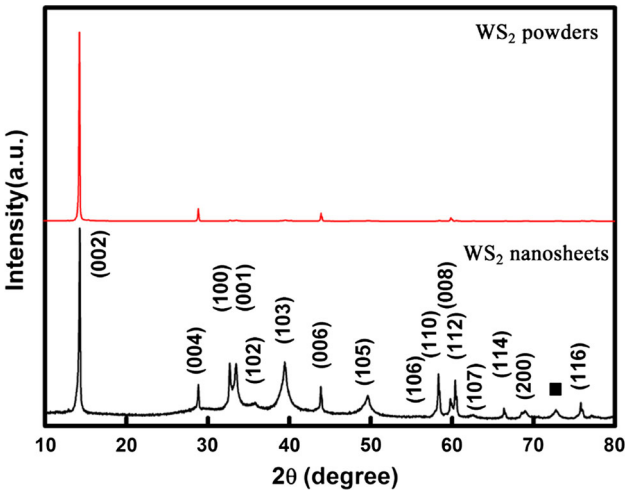

Figure 3 The XRD patterns of the exfoliated WS_2 nanosheets and commercial WS_2 powders.

(SEM), transmission electron microscopy (TEM), high-resolution transmission electron microscopy (HRTEM), atomic force microscopy (AFM), and Raman scattering.

Results and discussion

Figure 1 schematically depicts the formation processes of two-dimensional tungsten disulfide (WS_2) nanosheets produced by Li intercalation/exfoliation of layered bulk WS_2 via the solvothermal and sonication treatment, which is similar with the cases of Bi_2Te_3 [21], Bi_2Se_3 [23], and MoS_2 [15]. Briefly, because the bulk WS_2 layers are connected by weak van der Waals interaction, lithium atoms of Li_2CO_3 dissolved in benzyl alcohol can be easily intercalated into the interlayers of bulk WS_2 under appropriate solvothermal condition. When the Li-intercalated WS_2 were sonicated in the mixed solution of distilled water and DMF for 12 h, the lithium atoms between layers of bulk WS_2 were extracted out, leading to the production of the exfoliated WS_2 layers. Finally, two-dimensional WS_2 nanosheets powders were collected from the suspension by centrifuging.

As shown in Fig. 2a, b, the morphologies of bulk WS_2 and the exfoliated WS_2 layers are characterized by SEM. It can be obviously observed that the bulk WS_2 precursor consists of many thick plates with native layered structure. On the contrary, the exfoliated products are thin two-dimensional WS_2 nanosheets with flat and smooth surfaces. There is no distinct difference in the lateral sizes of the synthesized WS_2 nanosheets and the starting bulk WS_2 plates.

Figure 3 shows the XRD patterns of the exfoliated WS_2 products and commercial WS_2 powders. The main reflections of the WS_2 nanosheets can be well indexed to hexagonal 2H-WS_2 with lattice constants of $a = 3.1532$ Å and $c = 12.323$ Å (ICDD PDF Card No. 08-0237) except for an unknown peak marked by square. The sharp profiles of the reflections suggest good crystallization of the sample. Compared with the XRD pattern of the commercial WS_2 powders, the exfoliated WS_2 products show the same crystal structure except for the size-related broadening of the reflections.

Figure 4a, b shows the low-magnification TEM images of exfoliated WS_2 nanosheets. The individual WS_2 nanosheets are randomly stacked and look transparent under the irradiation of electron beam, which implies that the obtained WS_2 nanosheets are very thin. Microstructures of the WS_2 nanosheets are

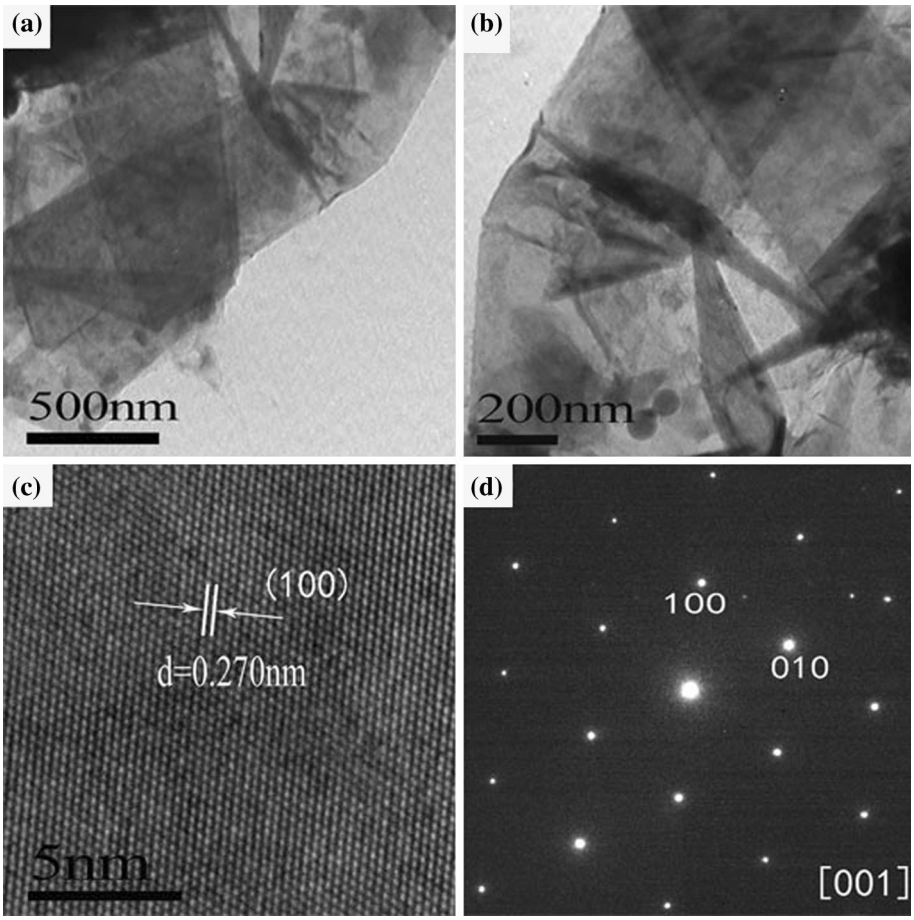

Figure 4 **a**, **b** Low-magnification TEM images of the exfoliated WS_2 nanosheets. **c** High-resolution TEM (HRTEM) image and SAED pattern (**d**) of the as-prepared WS_2 nanosheets.

further checked by HRTEM. Representative HRTEM crystal lattice images taken from the as-prepared samples are shown in Fig. 4c. Clear lattice fringes with a spacing of 0.270 nm shown in the HRTEM image can be indexed to the {100} plane of 2H-WS_2, revealing the single-crystal nature of the prepared nanosheets. The well-arranged lattice with hexagonal symmetry indicates that the top surface of the nanosheet is {001} plane. The SAED pattern shown in Fig. 4d can be indexed to 2H-WS_2, further demonstrating the nanosheet is well-crystallized single crystal. The zone axis of the SAED pattern is along [001], which reveals the [001] preferential orientation of the nanosheet, too.

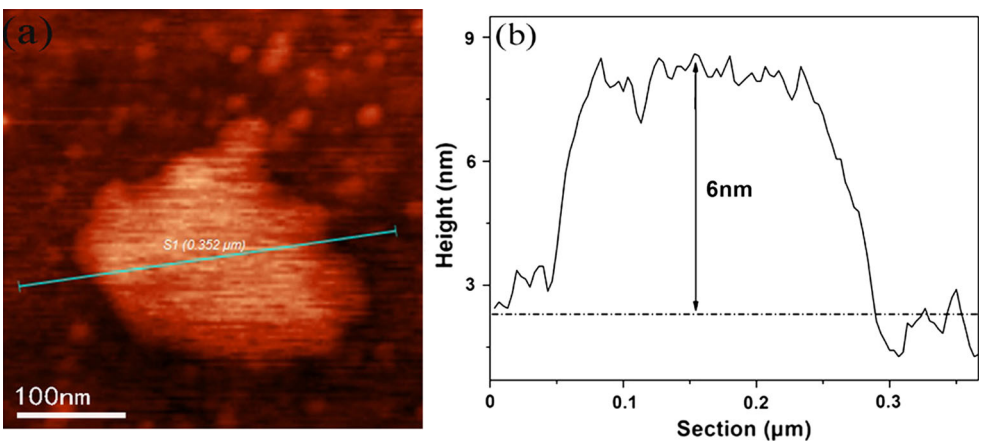

Figure 5 **a** Typical AFM image of the exfoliated WS_2 nanosheet. **b** Height profile corresponding to the *dashed line* in the image of the exfoliated WS_2 nanosheet.

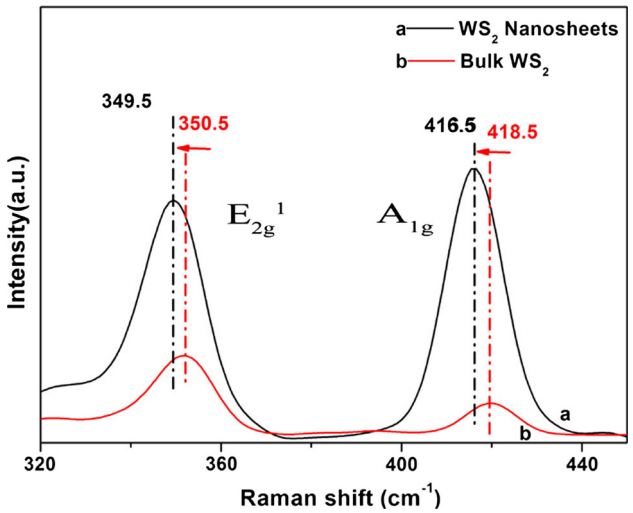

Figure 6 Raman spectra for WS_2 nanosheets (*a*) and WS_2 bulk (*b*).

As shown in Fig. 5a, a typical AFM topography image is shown to confirm the thickness of the as-prepared nanosheets. The nanosheet has smooth and flat surface with a uniform thickness across the lateral dimension. Figure 5b shows the height profile of the nanosheet. It can be seen that the WS_2 nanosheet has a thicknesses of about 6 nm, which corresponds to about 8 times the thickness of WS_2 monolayer [24].

Room-temperature Raman spectrum of the prepared WS_2 nanosheets (Fig. 6) shows two peaks at 349.5 and 416.5 cm^{-1}, which can be assigned to E^1_{2g} and A_{1g} phonon modes of 2H-WS_2 [11], respectively. Compared with the corresponding phonon modes of bulk WS_2 shown in Fig. 6, there is slightly redshifts in those of nanosheets. It is known that A_{1g} and E^1_{2g} modes are due to the vibrations perpendicular and parallel to the *S–W–S* layer, respectively [11, 25]. A_{1g} mode is sensitive to the thickness of WS_2 nanosheets, and the observed redshifts are consistent with the previous reports on the few-layer WS_2 [11, 24, 25] which indicates the weakened interaction between WS_2 layers with decreasing the thickness. On the other hand, E^1_{2g} mode has less dependence on the thickness and is thought to be influenced by the long-range Coulomb interactions [25]. The frequency difference of the two modes of the prepared WS_2 nanosheets is smaller than that of bulk WS_2, which also demonstrates their decreased thicknesses [11].

Conclusions

In summary, thin two-dimensional tungsten disulfide (WS_2) nanosheets have been successfully produced by Li intercalation/exfoliation of bulk WS_2 via solvothermal technique. The as-prepared WS_2 nanosheets are high-quality single crystals with hexagonal structure and have thin thicknesses of few-layer WS_2. The work provides a facile and efficient route to large-scale preparation of two-dimensional WS_2 nanosheets with potential applications in optoelectronic nanodevices.

Acknowledgements

This work was financially supported by the Natural Science Foundation for Distinguished Young Scholars of Xinjiang (Grant No. 2013711007).

Compliance with ethical standards

Conflict of interest The authors declare that they have no conflict of interest.

References

[1] Geim AK, Novoselov KS (2007) The rise of grapheme. Nat Mater 6:183–191. doi:10.1038/nmat1849

[2] Geim AK (2009) Graphene: status and prospects. Science 324:1530–1534. doi:10.1126/science.1158877

[3] Rao CNR, Sood AK, Angew Subrahmanyam KS, Govindaraj A (2009) Graphene: the new two-dimensional nanomaterial. Chem Int Ed 48:7752–7777. doi:10.1002/anie.200901678

[4] Rao CNR, Sood AK, Subrahmanyam KS, Govindaraj A (2009) Graphene: the new two-dimensional nanomaterial. Angew Chem 121:7890–7916. doi:10.1002/anie.200901678

[5] Novoselov KS, Jiang D, Schedin F et al (2005) Two-dimensional atomic crystals. Proc Natl Acad Sci USA 102:10451–10453. doi:10.1073/pnas.0502848102

[6] Ramakrishna Matte HSS, Gomathi A, Manna Arun K, Late Dattatray J et al (2010) MoS_2 and WS_2 analogues of graphene. Angrew Chem Int Ed 49:4059–4062. doi:10.1002/anie.201000009

[7] Rao CNR, Nag A, Eur J (2010) Inorganic analogues of graphene. J Inorg Chem 27:4244–4250. doi:10.1002/ejic.201000408

[8] Nag A, Raidongia K, Hembram KPSS et al (2010) Graphene analogues of BN: novel synthesis and properties. ACS Nano 4:1539–1544. doi:10.1021/nn9018762

[9] Katsnelson MI (2007) Graphene: carbon in two dimensions. Mater Today 10:20–27. doi:10.1016/S1369-7021(06)71788-6

[10] Komsa H-P, Krasheninnikov AV (2012) Two dimensional transition metal dichalcogenide alloys: stability and electronic properties. J Phys Chem Lett 3:3652–3656. doi:10.1021/jz301673x

[11] Gutiérrez HR, Perea-López N, Elías AL et al (2013) Extraordinary room-temperature photoluminescence in triangular WS_2 monolayers. Nano Lett 13:3447–3454. doi:10.1021/nl3026357

[12] Eda G, Yamaguchi H, Voiry D et al (2011) Photoluminescence from chemically exfoliated MoS_2. Nano Lett 11:5111–5116. doi:10.1021/nl201874w

[13] Korn T, Heydrich S, Hirmer M et al (2011) Low-temperature photocarrier dynamics in monolayer MoS_2. Appl Phys Lett 99:102109. doi:10.1063/1.3636402

[14] Radisavljevic B, Radenovic A, Brivio J et al (2011) Single-layer MoS_2 transistors. Nat Nanotechnol 6:147–150. doi:10.1038/nnano.2010.279

[15] Liu YD, Ren L, Qi X et al (2013) Preparation, characterization and photoelectrochemical property of ultrathin MoS_2 nanosheets via hydrothermal intercalation and exfoliation route. J Alloys Compd 571:37–42. doi:10.1016/j.jallcom.2013.03.031

[16] Lee HS, Min SW, Chang YG et al (2012) MOS_2 nanosheet phototransistors with thickness-modulated optical energy gap. Nano Lett 12:3695–3700. doi:10.1021/nl301485q

[17] Li Yadong, Li Xiaolin, He Rongrui et al (2002) Artificial lamellar mesostructures to WS_2 nanotubes. J Am Chem Soc 124:1411–1416. doi:10.1021/ja012055m

[18] Li XL, Ge JP, Li YD (2004) Atmospheric pressure chemical vapor deposition: an alternative route to large-scale MOS_2 and WS_2 inorganic fullerene-like nanostructures and nanoflowers. Chem Eur J 10:6163–6171. doi:10.1002/chem.200400451

[19] Elías AL, Perea-López N, Castro-Beltrán A et al (2013) Controlled synthesis and transfer of large-area WS_2 sheets: from single layer to few layers. ACS Nano 7:5235–5242. doi:10.1021/nn400971k

[20] Wang Y, Zhou C, Wang W et al (2013) Preparation of two dimensional atomic crystals bn, WS_2, and MoS_2 by supercritical CO_2 assisted with ultrasound. Ind Eng Chem Res 52:4379–4382. doi:10.1021/ie303633c

[21] Huang K-J, Liu Y-J, Wang H-B et al (2014) Signal amplification for electrochemical DNA biosensor based on two-dimensional graphene analogue tungsten sulfide–grapheme composites and gold nanoparticles. Sens Actuators B 191:828–836. doi:10.1016/j.snb.2013.10.072

[22] Ren L, Qi X, Liu Y et al (2012) Large-scale production of ultrathin topological insulator bismuth telluride nanosheets by a hydrothermal intercalation and exfoliation route. J Mater Chem 22:4921–4926. doi:10.1039/C2JM15973B

[23] Sun Y, Cheng H, Gao S et al (2012) Atomically thick bismuth selenide freestanding single layers achieving enhanced thermoelectric energy harvesting. J Am Chem Soc 134:20294–20297. doi:10.1021/ja3102049

[24] Zhang Y, Zhang Y, Ji Q et al (2013) Controlled growth of high-quality monolayer WS_2 layers on sapphire and imaging its grain boundar. ACS Nano 7:8963–8971. doi:10.1021/nn403454e

[25] Berkdemir A, Gutiérrez HR et al (2013) Identification of individual and few layers of WS_2 using Raman spectroscopy. Sci Rep 3:1–8. doi:10.1038/srep01755